NATIONAL ADVISORY COMMITTEE FOR AERONAUTICS

REPORT No. 161

THE DISTRIBUTION OF LIFT OVER WING TIPS AND AILERONS

By DAVID L. BACON

WASHINGTON
GOVERNMENT PRINTING OFFICE
1923

AERONAUTICAL SYMBOLS.

1. FUNDAMENTAL AND DERIVED UNITS.

	Symbol.	Metric.		English.	
		Unit.	Symbol.	Unit.	Symbol.
Length...	l	meter.....	m.	foot (or mile).....	ft. (or mi.).
Time.....	t	second.....	sec.	second (or hour).....	sec. (or hr.).
Force....	F	weight of one kilogram.....	kg.	weight of one pound....	lb.
Power...	P	kg.m/sec.....	.....	horsepower.....	HP
Speed....	.....	m/sec.....	m. p. s.	mi/hr.....	M. P. H.

2. GENERAL SYMBOLS, ETC.

Weight, $W=mg$.

Standard acceleration of gravity, $g=9.806\text{m/sec.}^2=32.172\text{ft/sec.}^2$

Mass, $m=\frac{W}{g}$

Density (mass per unit volume), ρ

Standard density of dry air, 0.1247 (kg.-m.-sec.) at 15.6°C. and 760 mm. = 0.00237 (lb.-ft.-sec.)

Specific weight of "standard" air, 1.223 kg/m.^{3} = 0.07635 lb/ft.^{3}

Moment of inertia, mk^2 (indicate axis of the radius of gyration, k, by proper subscript).

Area, S; wing area, S_w, etc.

Gap, G

Span, b; chord length, c.

Aspect ratio $=b/c$

Distance from c. g. to elevator hinge, f.

Coefficient of viscosity, μ.

3. AERODYNAMICAL SYMBOLS.

True airspeed, V

Dynamic (or impact) pressure, $q=\frac{1}{2}\rho V^2$

Lift, L; absolute coefficient $C_L=\frac{L}{qS}$

Drag, D; absolute coefficient $C_D=\frac{D}{qS}$.

Cross-wind force, C; absolute coefficient $C_c=\frac{C}{qS}$.

Resultant force, R

(Note that these coefficients are twice as large as the old coefficients L_c, D_c.)

Angle of setting of wings (relative to thrust line), i_w

Angle of stabilizer setting with reference to thrust line i_t

Dihedral angle, γ

Reynolds Number $=\rho\frac{Vl}{\mu}$, where l is a linear dimension.

e. g., for a model airfoil 3 in. chord, 100 mi/hr., normal pressure, 0°C: 255,000 and at 15.6°C, 230,000;

or for a model of 10 cm. chord, 40 m/sec., corresponding numbers are 299,000 and 270,000.

Center of pressure coefficient (ratio of distance of C. P. from leading edge to chord length), C_p.

Angle of stabilizer setting with reference to lower wing. $(i_t-i_w)=\beta$

Angle of attack, α

Angle of downwash, ϵ

REPORT No. 161

THE DISTRIBUTION OF LIFT OVER WING TIPS AND AILERONS

By DAVID L. BACON

National Advisory Committee for Aeronautics

20371—23——1

REPORT No. 161.

THE DISTRIBUTION OF LIFT OVER WING TIPS AND AILERONS.[1]

By David L. Bacon.

SUMMARY.

This investigation was carried out in the 5-foot wind tunnel of the Langley Memorial Aeronautical Laboratory for the purpose of obtaining more complete information than was heretofore available on the distribution of lift between the ends of wing spars, the stresses in ailerons, and the general subject of airflow near the tip of a wing.

It includes one series of tests on four models without ailerons, having square, elliptical, and raked tips respectively, and a second series of positively and negatively raked wings with ailerons adjusted to different settings.

The results show that negatively raked tips give a more uniform distribution of air pressure than any of the other three arrangements, because the tip vortex does not disturb the flow at the trailing edge. Aileron loads are found to be decidedly less severe on wings with negative rake than on those with positive rake. The data are presented in such form as to permit direct application to the calculation of aileron and wing stresses and also to facilitate the proper distribution of load in sand testing. Contour charts show in great detail the complex distribution of lift over the wing.

INTRODUCTION.

The choice of wing tip forms has in the past been largely a matter of personal preference, a large variety of shapes being found on up-to-date machines. The few attempts to determine the most desirable form by measurements of lift and drag were inconclusive, but it has been repeatedly shown by experiments with ailerons and with airflow phenomena that the effect of wing tip shape on controllability and on spar stresses is by no means negligible. The present research was therefore undertaken with the object of throwing additional light on the complex distribution of the air loads which occur on wing tips of various forms.

METHODS AND APPARATUS.

The method was to measure, by means of a multiple manometer, the pressure distribution over certain aerofoils when held in a wind tunnel. The N. A. C. A. 73 aerofoil which had previously shown excellent performance (N. A. C. A. report No. 152) was used for each of these tests. This is a double convex aerofoil having at the center section a maximum thickness of 22.1 per cent of the chord and tapered to a thickness of 5.51 per cent of the chord at the tip. (See fig. 1.) The models for this research had a chord of 153 mm. (6 inches) and a mean semi-span of 457 mm. (18 inches). An air speed of 30 m./sec. (67.2 m. p. h.) was used, giving a Vl of 4.59 m.^{2}/sec. (33.6 m. p. h. $\times$ ft. or 49.3 ft.^{2}/sec.) and a Reynolds number of approximately 300,000.

Four models were used, one square, one elliptical, and one each with positive and negative rake (fig. 2); the latter were also fitted with ailerons. The ordinates of all sections of the elliptical and raked tips were proportional to the lengths of their corresponding chords. Because of the thick section the models were made of laminated wood, grooved with air passages and finished with a smooth paper covering as described in N. A. C. A. report No. 150.

It is of course desirable in such tests to use the largest scale of model which can be tested without excessive interference from the tunnel walls, and for this reason the system described in British Advisory Committee for Aeronautics R. & M. No. 347 was adopted.

[1] In this paper the term "lift" is used with a meaning slightly different from the definition given in the N. A. C. A Nomenclature for Aeronautics. The lift as indicated in this paper is measured normal to the wind chord, not normal to the flight path of the airplane. The numerical difference between the lift as measured normal to the flight path and normal to the wing chord is very small.

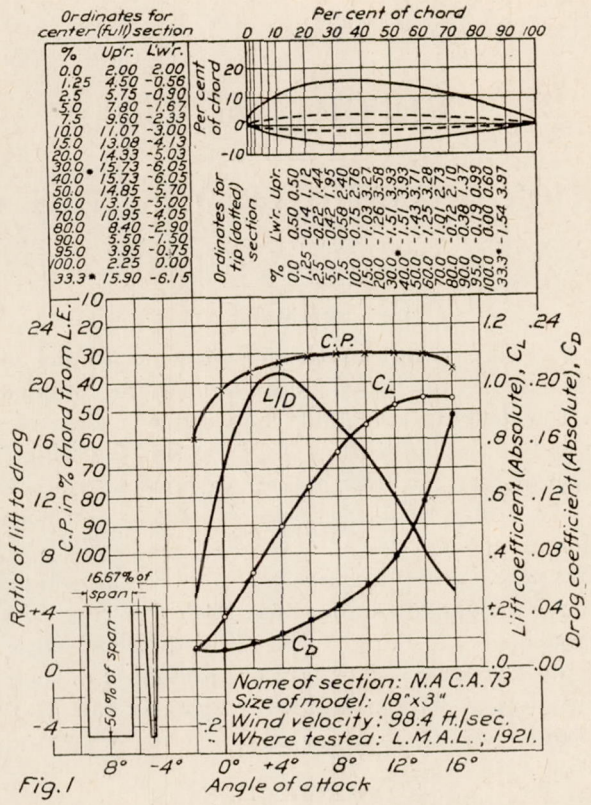

Fig. 1

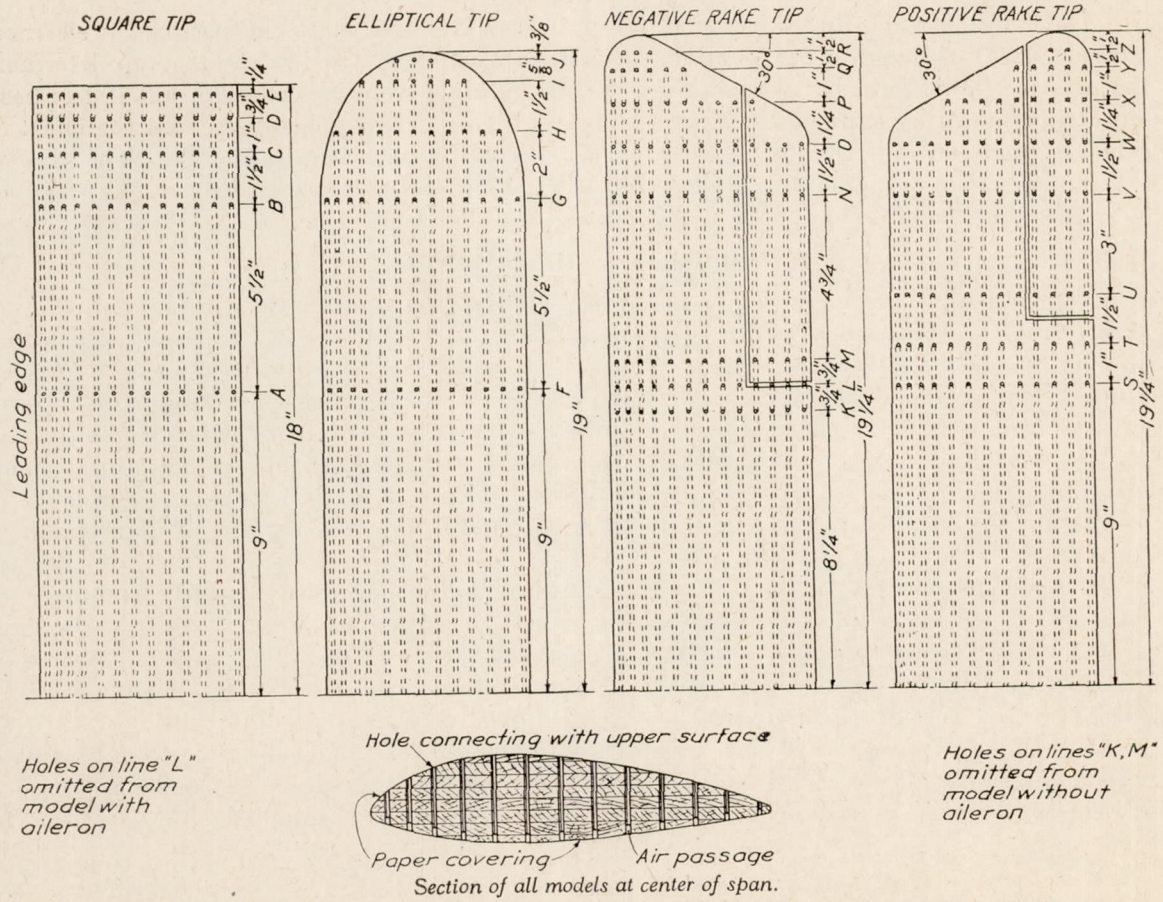

Section of all models at center of span.

FIG. 2.—Plan form and maximum section of models used in the experiments, showing location of pressure holes.

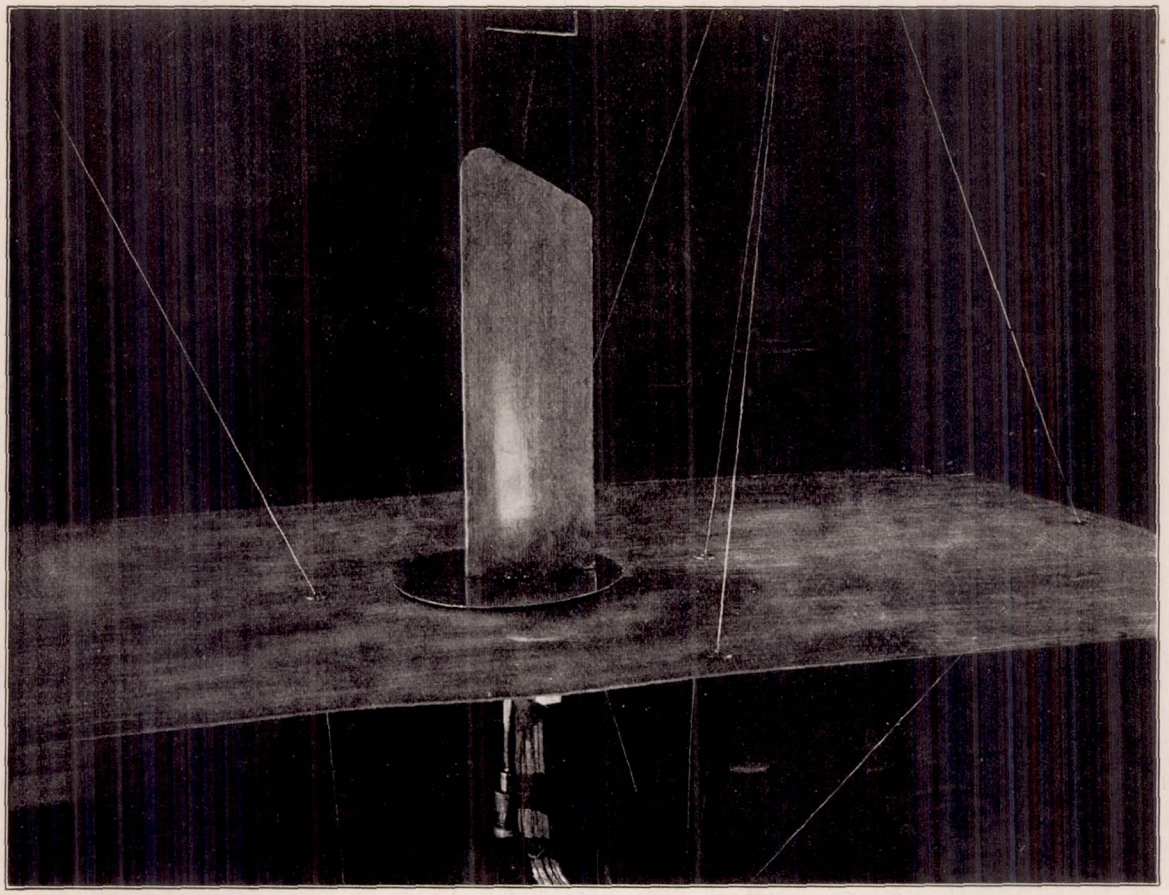

FIG. 3.—Model set up for test.

By using only one side of an entire wing, and by supporting a large and smooth flat plate at the center line of the wing and parallel to the air stream, the same air flow is obtained on that half of the model as would have been the case had a complete model been tested. It is therefore possible to practically double the chord of the aerofoil which may be tested in a tunnel of given diameter.

It has been previously demonstrated that the reflection method above described is satisfactory for the measurement of pressures on ordinary wings symmetrical about the X axis, the use of ailerons, however, renders the model unsymmetrical and thereby introduces an element of error in that the resulting inter-aileron interference corresponds to that of two ailerons both down, or both up, and is therefore the opposite of that which would actually occur in practice. It is improbable, however, that the error thus introduced in these experiments is of perceptible magnitude.

The combined error in the original pressure measurements, due to faulty contours and misalignment of wing, speed fluctutations, and difficulty of reading manometer, are probably no greater than 5 per cent. The drawing of the original pressure curves and the fairing of the contour charts is to some extent dependent upon the judgment of the draftsman, though the large number of points minimizes error from this source. The mechanical integrations of areas and moments of area may be checked to within 2 per cent except for those curves composed of positive and negative loops where the net area is small and the relative accuracy correspondingly less.

RESULTS.

The observed distribution of pressures along the different chord stations of two models are shown in Figures 4 and 5. All curves of pressure on the lower surface of the wing are dotted, so as to minimize confusion. The ordinate corresponding to the dynamic pressure is indicated on the charts. It is deemed unnecessary to reproduce the complete series of these charts because the information is presented more conveniently in the contour maps, Figures 9 to 16 inclusive. The contours indicate the net pressure differences between the upper and lower surfaces of the wing at each point, plotted according to an arbitrary scale in which the dynamic pressure q is equal to 7.5. The contour interval in most cases is 1 unit, though in a few cases it has been found advisable to use intervals of one-half unit where the pressure differences were small. These additional contours are shown by dotted lines.

From the contour maps several three-dimensional models have been built up for lecture purposes; photographs of these are given in Figures 6, 7, and 8.

WINGS WITHOUT AILERONS.

Examining first charts 9 to 12 depicting the lift distribution at four angles of attack on each of four different shapes of wing tip, we see that the square tip gives rise at all angles of attack to two high lift areas, separated by approximately half a chord length at $\alpha = -2°$ and approaching each other with increase in angle of attack until at $\alpha = 16°$ they form a double peak of great intensity. Referring to Figure 4 we see that this is due to a heavy local suction on the upper surface, apparently caused by the core of the wing tip vortex.[1] The positively raked tip also shows a region of very high lift near the extreme tip, but having a single rather than a double peak. A similar tendency is seen on the elliptical tip at high angles of attack—though in less pronounced form—the region of high lift merely enlarging in area and not building up in intensity. The negatively raked wing is comparatively free from these localized lifts and for all positive angles of attack exhibits remarkably smooth contours, with no regions of high lift except the usual one along the leading edge.

WINGS WITH AILERONS.

The usual aileron location is subject to the influence of the intense localized loads which occur on positively raked wings, the down aileron accentuating the magnitude of the suction on the upper surface. The maximum lift per unit length on the positively raked aileron at 0° angle of attack is more than twice that on the one negatively raked. This irregular distribution imposes unnecessary stresses on the aileron structure. The negatively raked ailerons exhibit a nearly constant loading over their entire length while the effect of the aileron on that part of the wing immediately in front of the hinge is also practically constant.

APPLICATION TO STRESS ANALYSIS.

The conventionalized assumptions of lift distribution now in use only roughly approximate the true conditions and if refinements of design are attempted it becomes necessary to determine the true distribution with greater exactitude than has heretofore been customary. If a pressure distribution chart is available it is a simple matter to determine the spar loads by mechanical methods and the greater exactitude of the results more than compensates for the few hours of work required.

For the purpose of comparison, the spar loads, shears, and bending moments have been derived for the positively and negatively raked wings at two angles of attack, the spars being arbitrarily located at 10 per cent and 65 per cent of the chord. The unit of pressure is taken as the dynamic pressure q and the unit of length as the chord c. The method consists in determining the area and center of area (or moment about the leading edge) for the curves of pressure distribution at each station, and solving for the reactions F and R at the spar positions (Fig. 17 and Tables I and II). These values are then plotted for the entire wing tip, using the distances

[1] R. & M. No. 197: The Flow of Air Round a Wing Tip.
N. A. C. A. Technical Report No. 83: Wind Tunnel Studies in Aerodynamic Phenomena at High Speed.

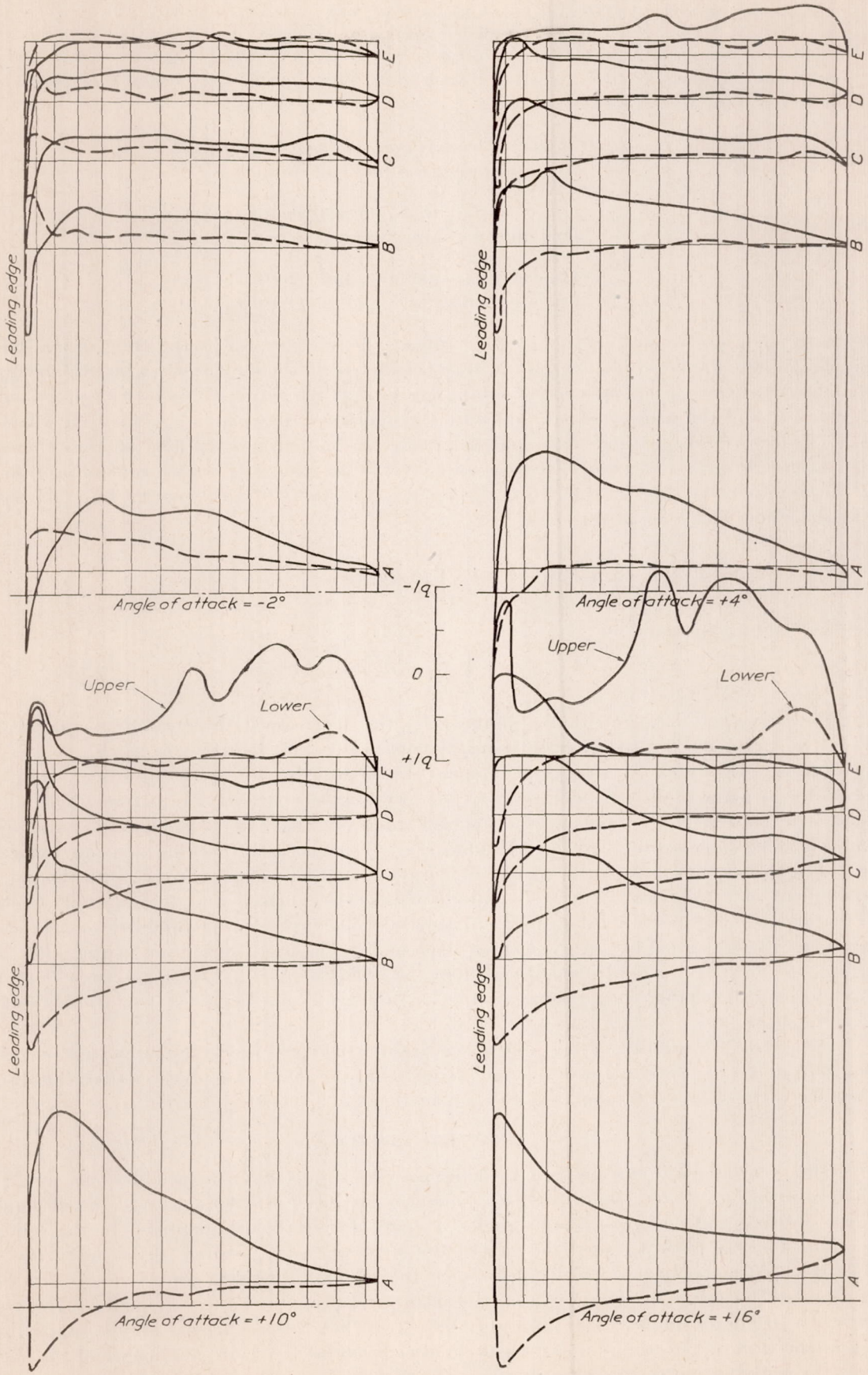

FIG. 4.—Pressure distribution along chord, without ailerons. Square tip.

of the stations from the wing tip as abscissae (Figs. 18–27); the resulting curves give the loci of the centers of pressure and the distribution along the span of the normal and spar loads. The ordinates may be expressed as follows:

$$C_N = \frac{\text{Load at section per unit length}}{\text{Dynamic pressure} \times \text{nominal chord}}.$$

$$F = \frac{\text{Load on front spar, per unit length}}{\text{Dynamic pressure} \times \text{nominal chord}}.$$

$$R = \frac{\text{Load on rear spar, per unit length}}{\text{Dynamic pressure} \times \text{nominal chord}}.$$

Both spars are treated as though they ran to the extreme tip of the wing, for although they do not actually do so, the tip loads will be transferred to them by other structural members. It is also assumed, for convenience in computation, that the chord of the aileron projected on the chord line of the wing does not vary with the aileron setting. It is obvious that whenever the C. P. locus crosses a spar that spar takes the whole load and the load on the other spar passes through zero. Also whenever the total load is zero the C. P. curve runs off to infinity.

If now we denote the distance from the tip of any section, in chord lengths, by y, the shears at that section may be expressed thus:

$$S_{\text{total}} = q \cdot c \int_o^y C_N \, dy; \; S_F = q \cdot c \int_o^y F \, dy; \text{ and } S_R = q \cdot c \int_o^y R \, dy$$

and the bending moments by

$$M_{\text{total}} = q \cdot c \int_o^y C_N \, y \, dy, \text{ etc.}$$

The curves of these functions, obtained by the mechanical integration of the lift distribution curves are printed directly beneath them in the same figures.

The application of the stress and moment curves will depend on the design and intended use of the airplane under consideration. They are intended particularly to throw light on the stresses in the overhung or cantilever portions of wings, and have not been carried nearer to the center lines of the machine than the mid point of the semispan. If the wing spars are externally braced nearer to the tip then this point, the curves should be compared only up to the point of attachment of the braces. The combinations of angles of attack and aileron angle likely to occur, and the air speed at that time—considering, of course, the possibilities of accelerated flight—will be governed by the type of airplane and the assumed discretion of the pilot. For fighting planes it is certainly wise to assume the extreme aileron movement coincident with the maximum probable wing loading, while for less active machines the conditions need not be so rigorous.

If we take, for example, a machine in which the wing spars are to be supported one chord length from the tip, the shears and bending moments at the point of support can be read directly from the curve sheets and tabulated for comparison as in Table II.

CONTROLLABILITY.

These curves may also be used to determine the rolling moment produced by any given aileron setting, by taking the sum of the moments produced about the axis of the airplane by equal positive and negative aileron angles on port and starboard ailerons. In the following computations we have assumed the axis of the airplane to be parrallel to the chord line, and that the central portion of the wing between the ailerons, does not contribute to the rolling moment. The latter assumption is amply justified by pressure measurements. The rolling moments are here computed for an aspect ratio of 6, but the coefficients may be applied with reasonable accuracy to wings of other aspect ratios provided the width and length of the ailerons bear a constant ratio to the wing chord.

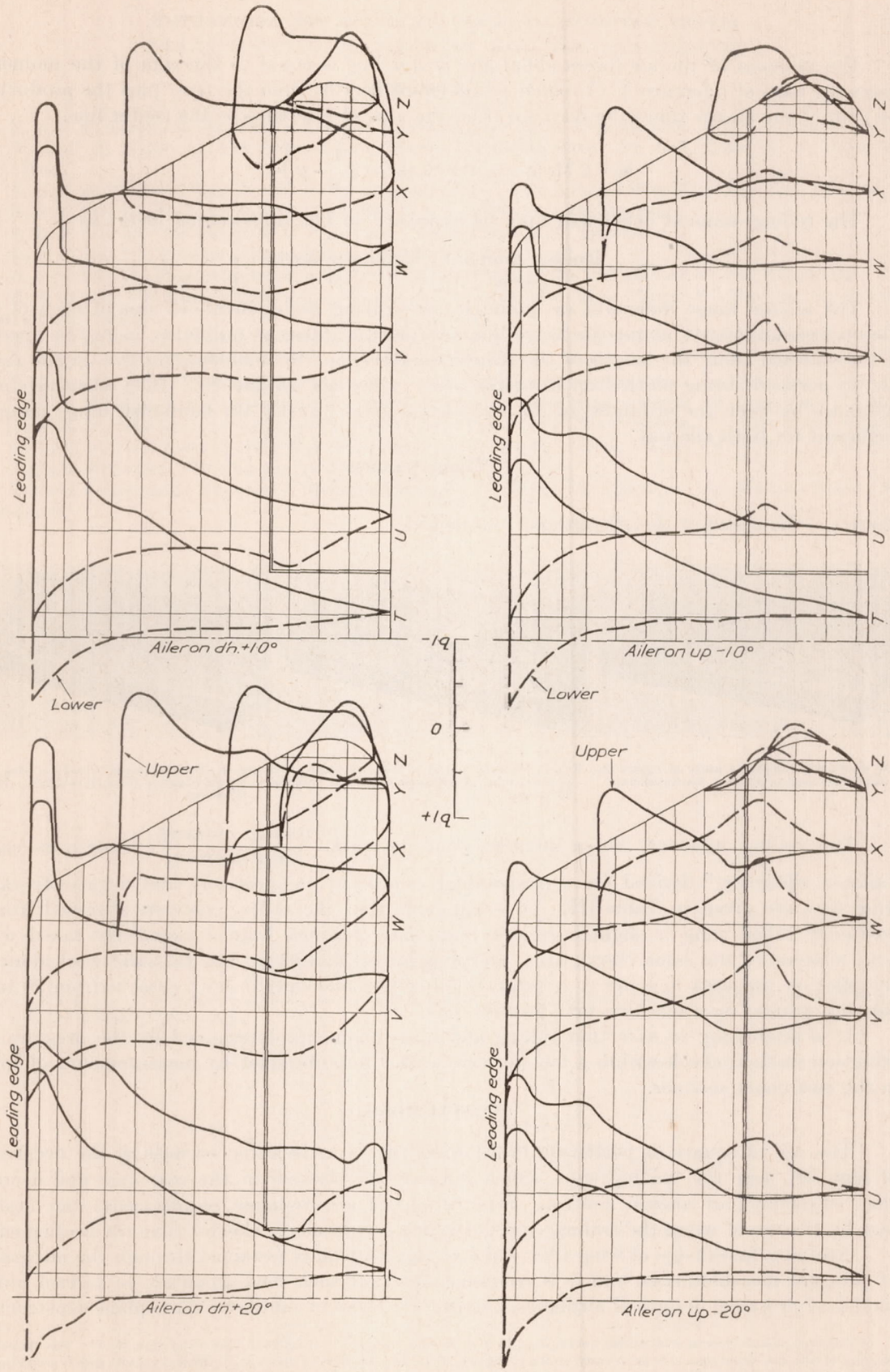

FIG. 5.—Pressure distribution along chord at +10° angle of attack, with ailerons. Positive rake.

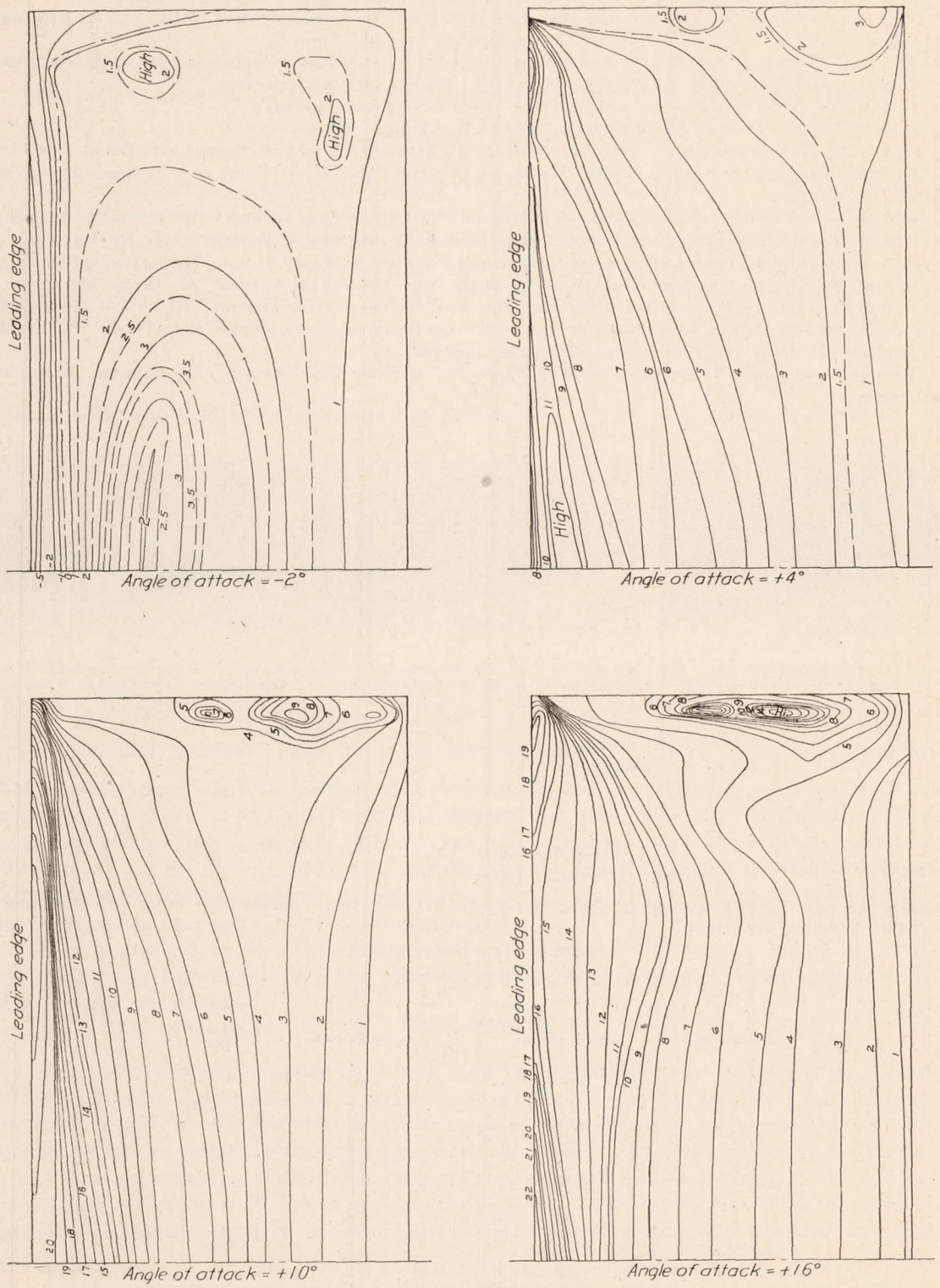

FIG. 9.—Square tip without aileron.

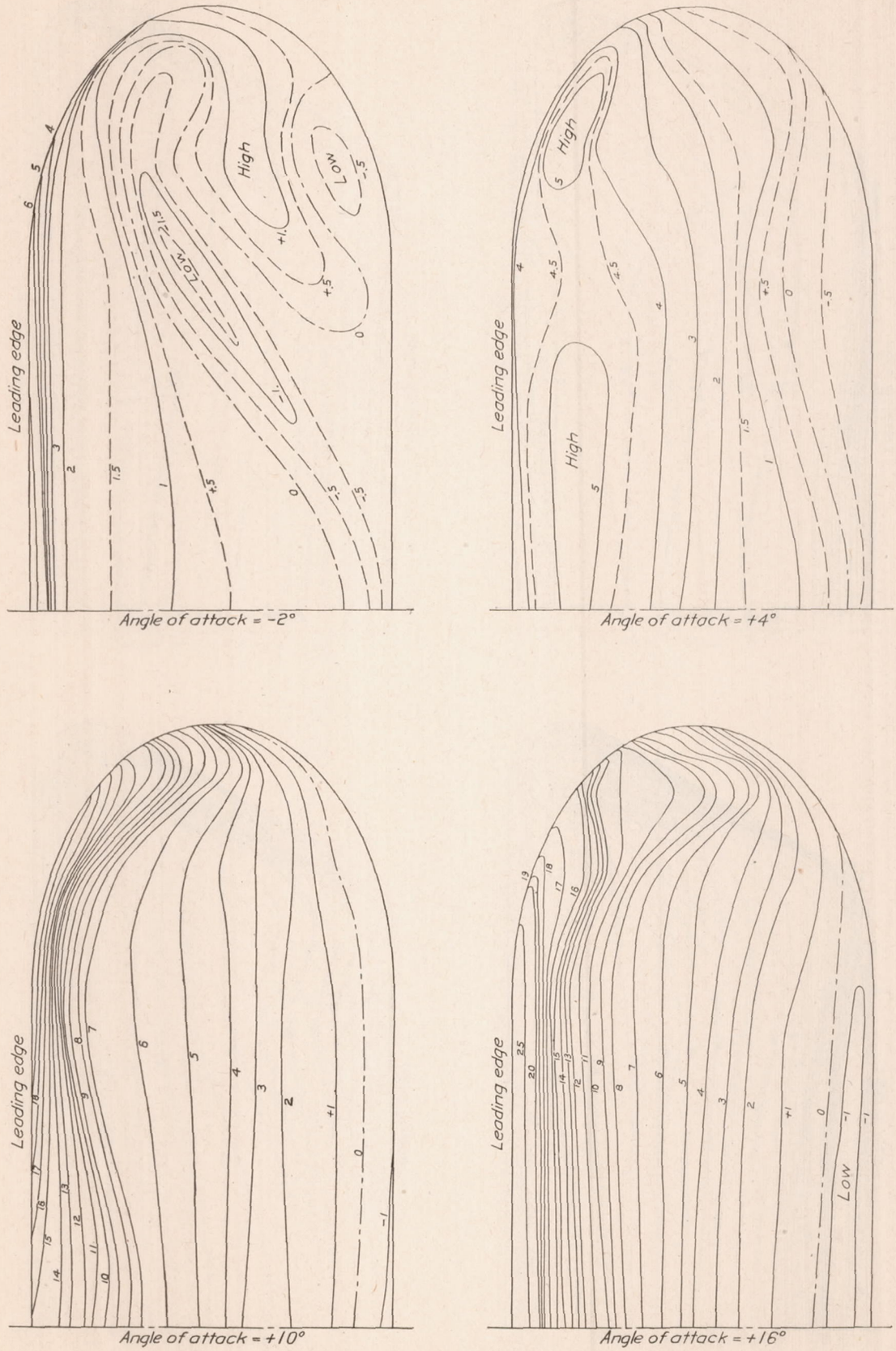

FIG. 10.—Elliptical tip without aileron.

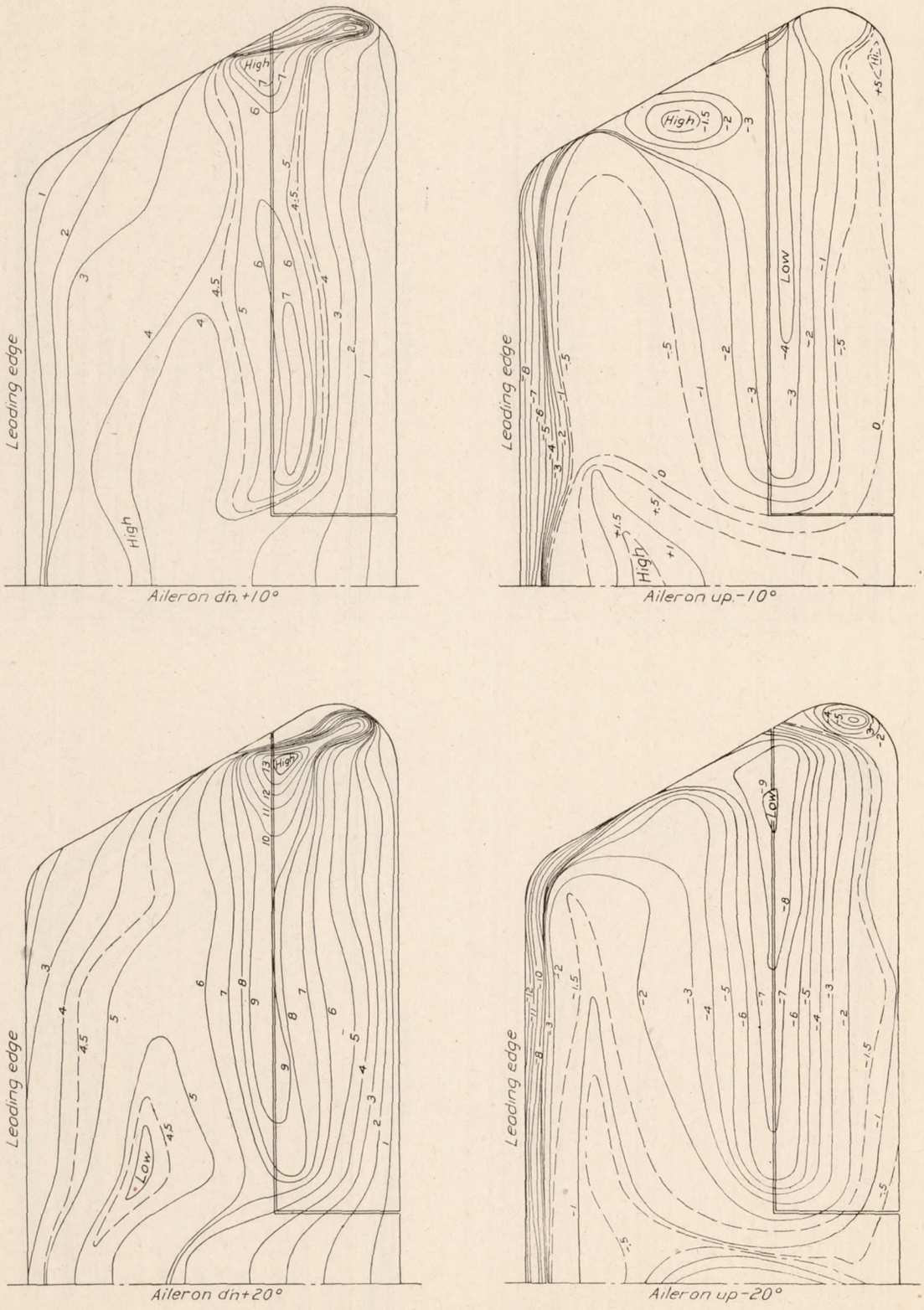

FIG. 13.—Positive rake at 0° angle of attack, with aileron.

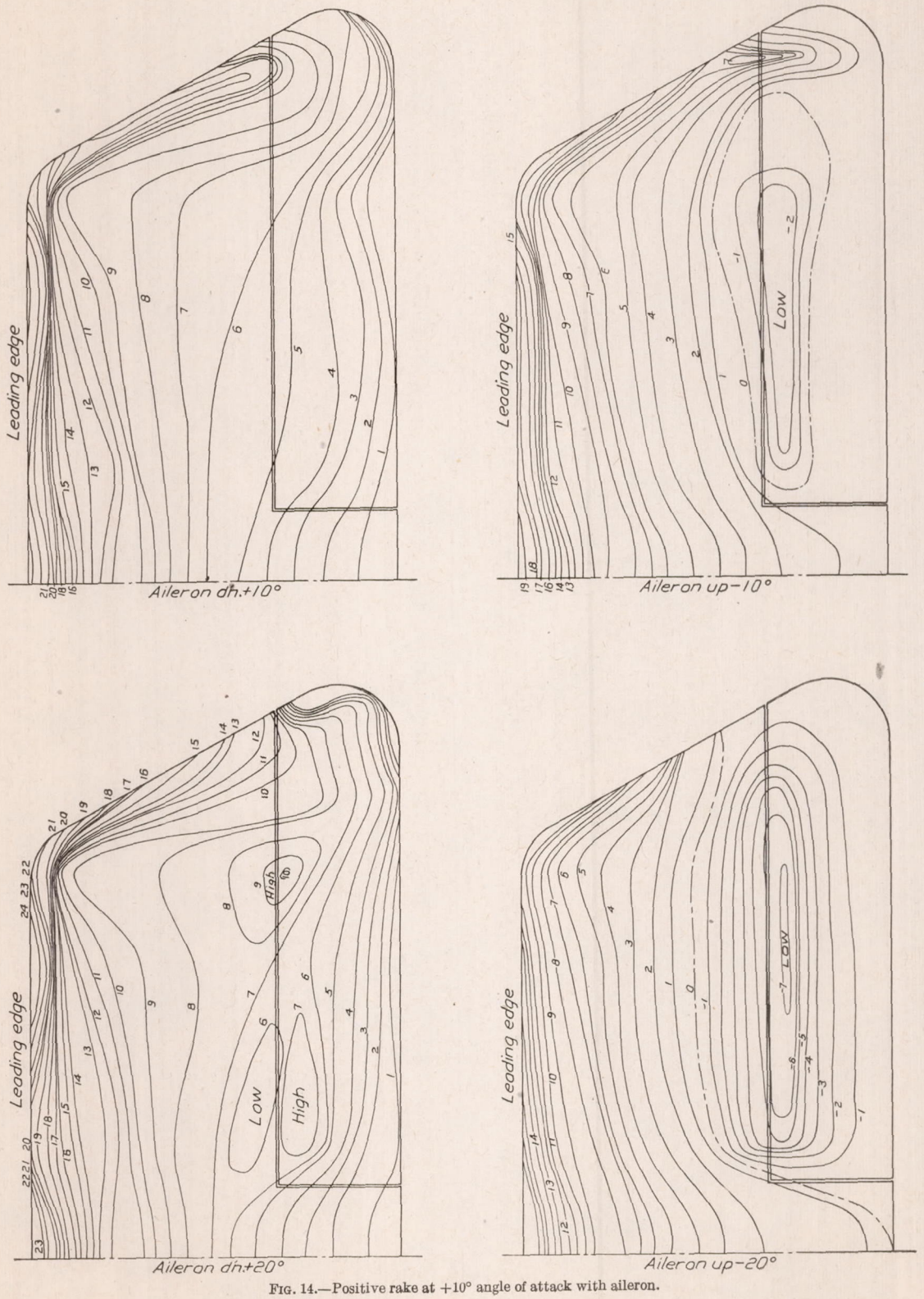

FIG. 14.—Positive rake at +10° angle of attack with aileron.

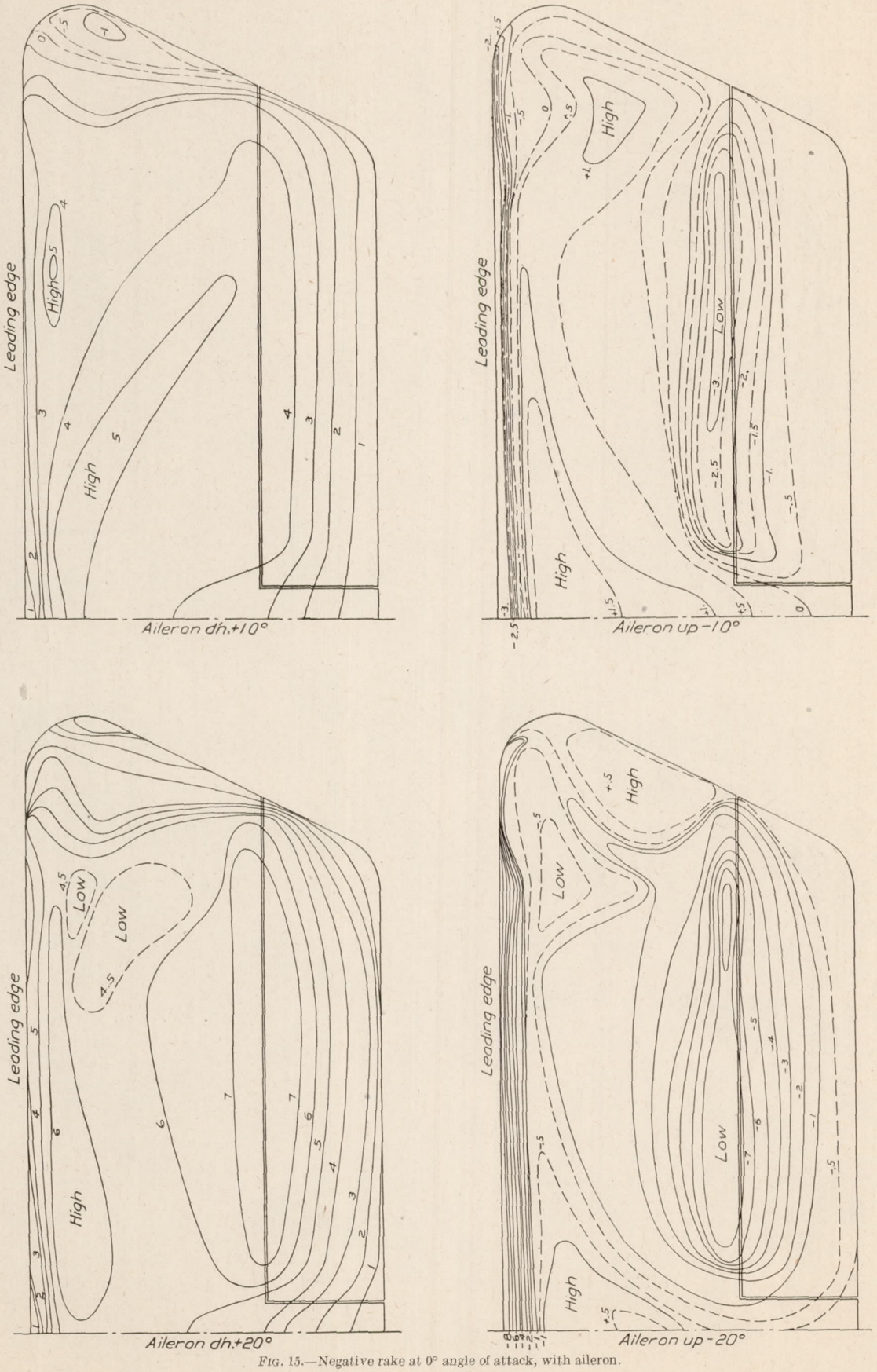

FIG. 15.—Negative rake at 0° angle of attack, with aileron.

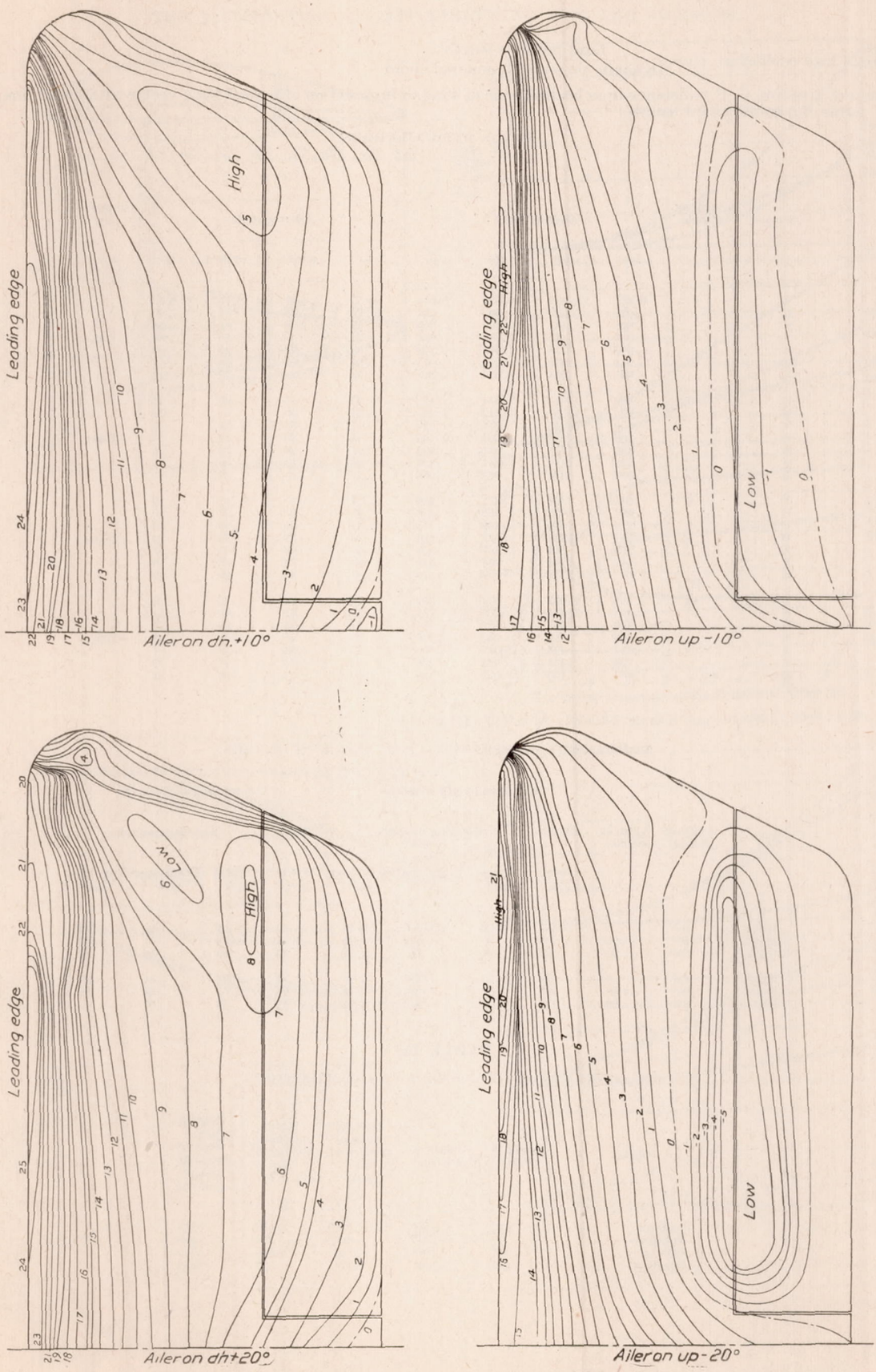

FIG. 16.—Negative rake at +10° angle of attack, with aileron.

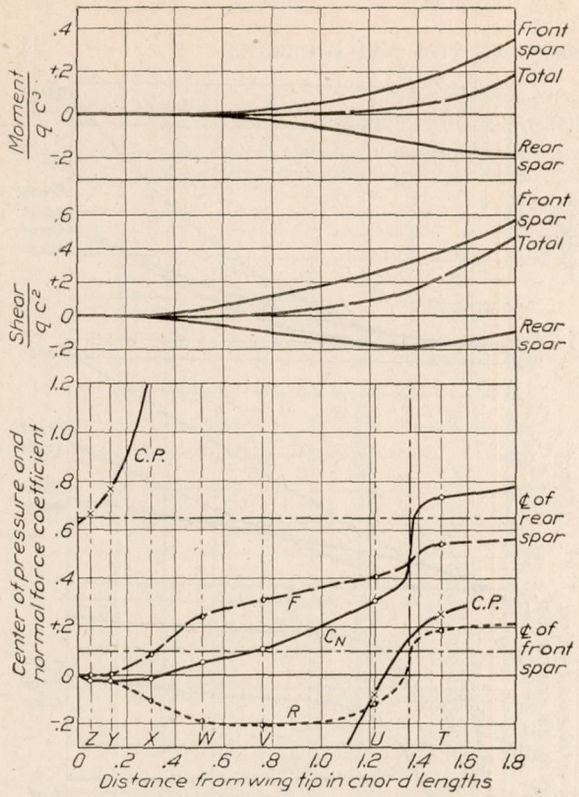

FIG. 21.—Positive rake at 10° angle of attack; aileron up −20°.

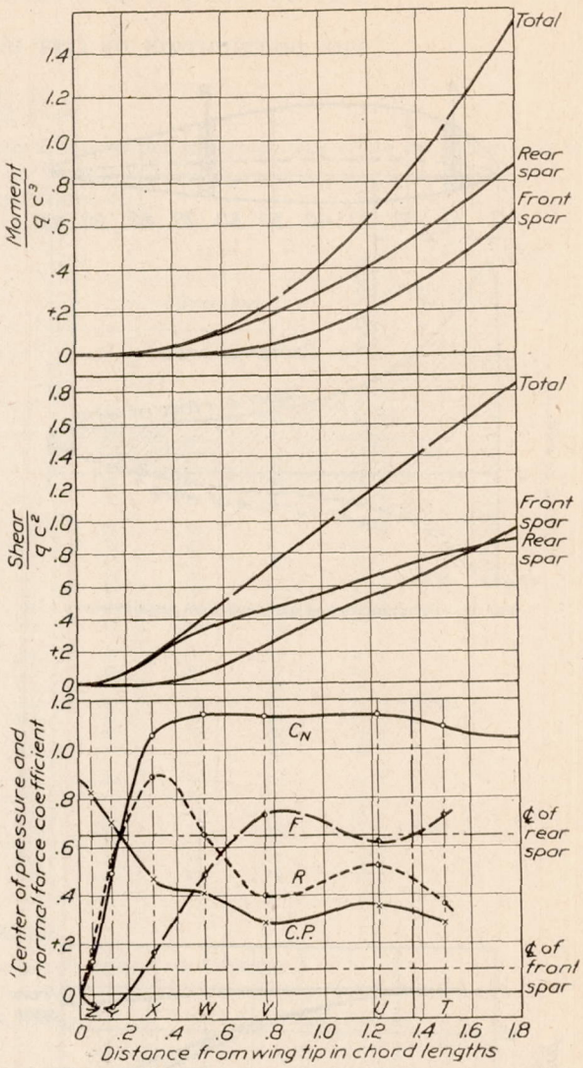

FIG. 22.—Positive rake at 10° angle of attack; aileron down +20°.

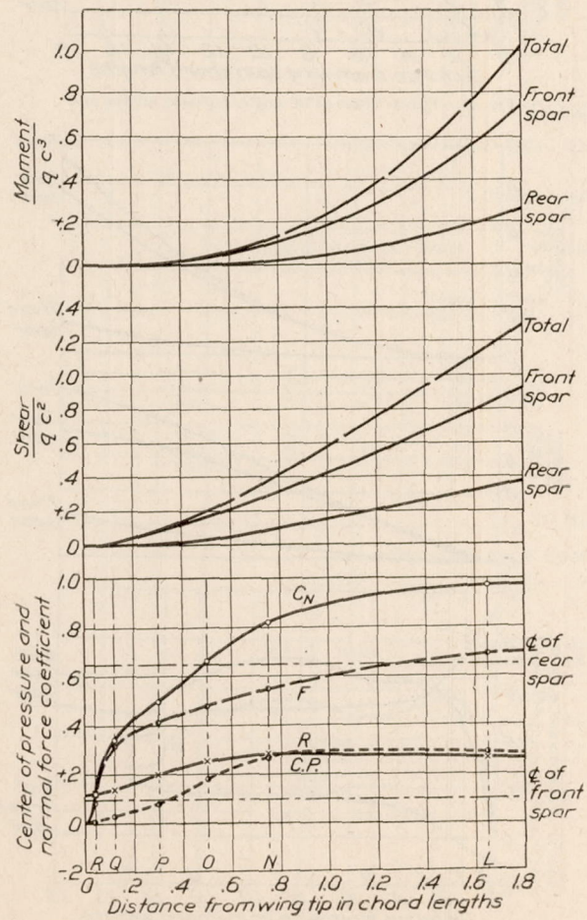

FIG. 23.—Negative rake at 10° angle of attack; aileron 0°.

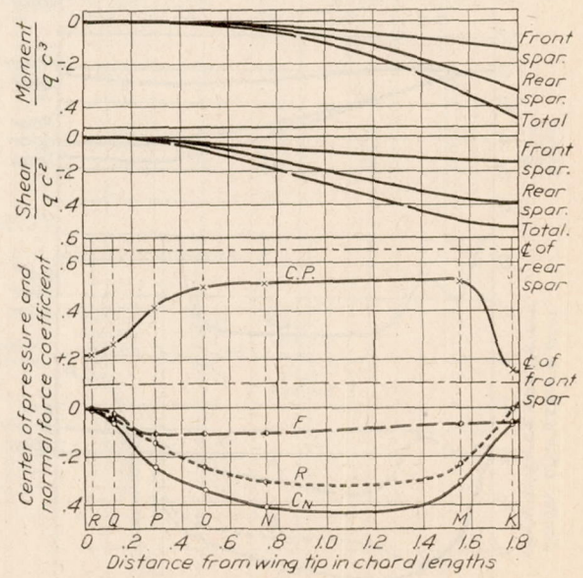

FIG. 24.—Negative rake at 0° angle of attack; aileron up −20°.

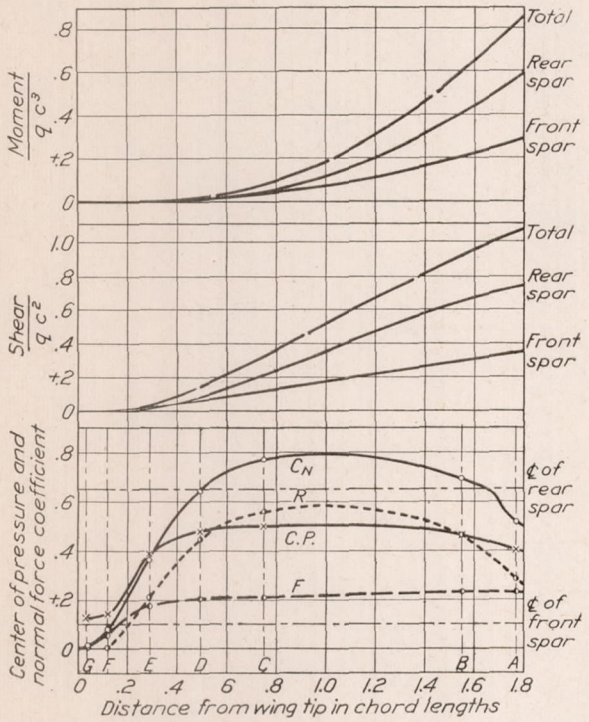

FIG. 25.—Negative rake at 0° angle of attack; aileron down +20°.

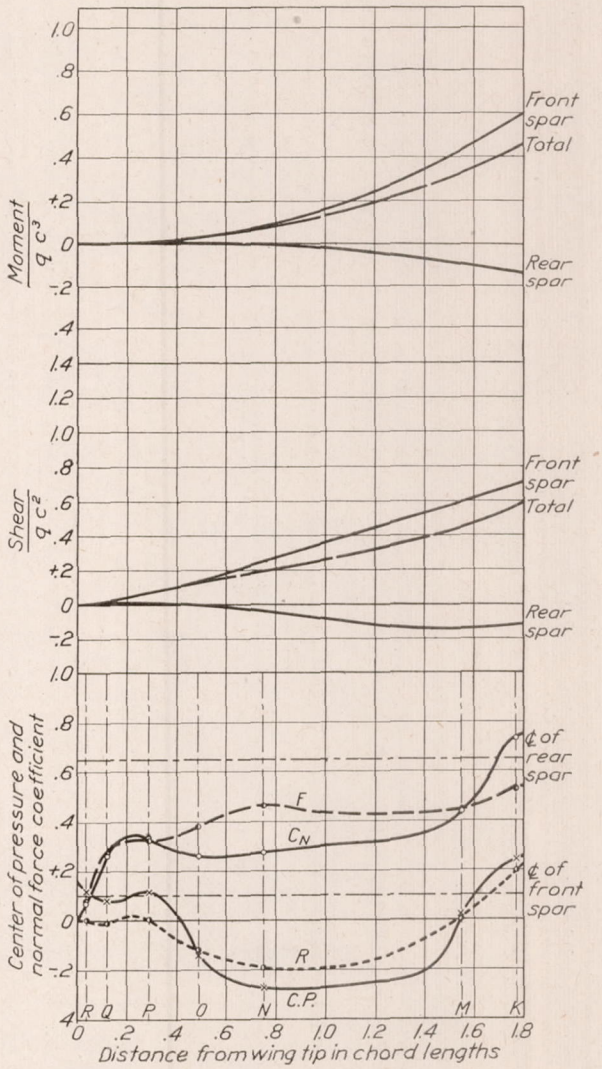

FIG. 26.—Negative rake at 10° angle of attack; aileron up −20°.

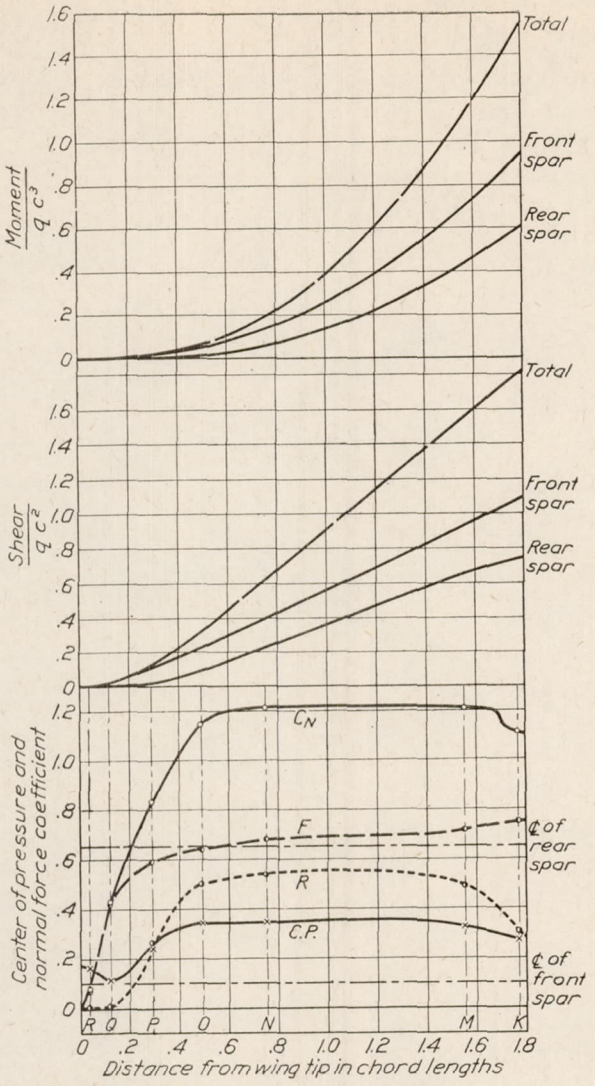

FIG. 27.—Negative rake at 10° angle of attack; aileron down +20°.

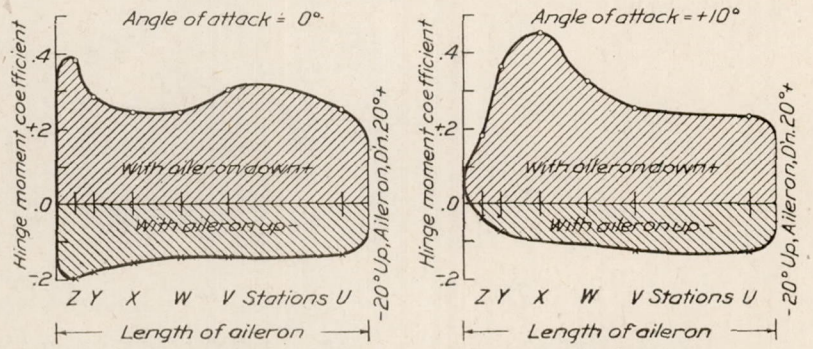

FIG. 28.—Distribution of moment along aileron hinge. Positive rake.

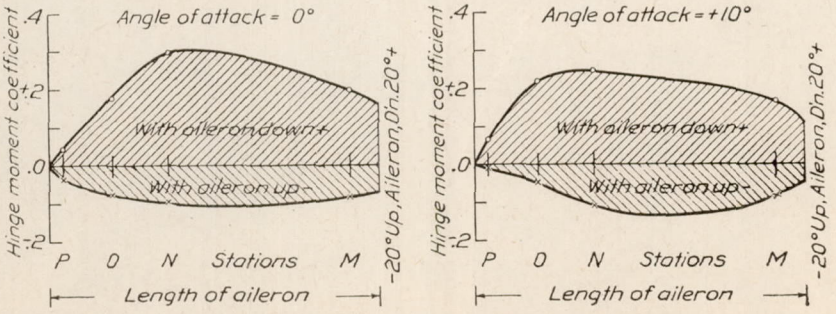

FIG. 29.—Distribution of moment along aileron hinge. Negative rake.

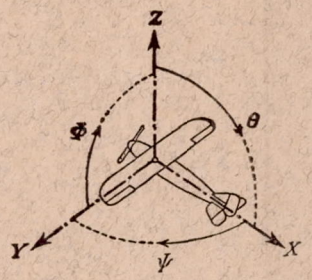

Positive directions of axes and angles (forces and moments) are shown by arrows.

Axis.		Force (parallel to axis) symbol.	Moment about axis.			Angle.		Velocities.	
Designation.	Symbol.		Designation.	Symbol.	Positive direction.	Designation.	Symbol.	Linear (component along axis).	Angular.
Longitudinal....	X	X	rolling.....	L	$Y \longrightarrow Z$	roll.....	Φ	u	p
Lateral.....	Y	Y	pitching...	M	$Z \longrightarrow X$	pitch....	Θ	v	q
Normal.....	Z	Z	yawing.....	N	$X \longrightarrow Y$	yaw.....	Ψ	w	r

Absolute coefficients of moment

$$C_l = \frac{L}{q\,b\,S} \quad C_m = \frac{M}{q\,c\,S} \quad C_n = \frac{N}{q\,f\,S}$$

Angle of set of control surface (relative to neutral position), δ. (Indicate surface by proper subscript.)

4. PROPELLER SYMBOLS.

Diameter, D

Pitch (a) Aerodynamic pitch, p_a
(b) Effective pitch, p_e
(c) Mean geometric pitch, p_g
(d) Virtual pitch, p_v
(e) Standard pitch, p_s

Pitch ratio, p/D

Inflow velocity, V'

Slipstream velocity, V_s

Thrust, T

Torque, Q

Power, P

(If "coefficients" are introduced all units used must be consistent.)

Efficiency $\eta = T\,V/P$

Revolutions per sec., n; per min., N

Effective helix angle $\Phi = \tan^{-1}\left(\frac{V}{2\pi r n}\right)$

5. NUMERICAL RELATIONS.

1 HP = 76.04 kg. m/sec. = 550 lb. ft/sec.
1 kg. m/sec. = 0.01315 HP
1 mi/hr. = 0.44704 m/sec.
1 m/sec. = 2.23693 mi/hr.

1 lb. = 0.45359 kg.
1 kg. = 2.20462 lb.
1 mi. = 1609.35 m. = 5280 ft.
1 m. = 3.28083 ft.